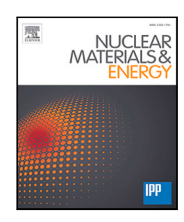
\$50 ELSEVIER

Contents lists available at ScienceDirect

Nuclear Materials and Energy

journal homepage: www.elsevier.com/locate/nme





Hydrogen permeation and retention in deuterium plasma exposed 316L ITER steel

A. Houben*, J. Scheuer, M. Rasiński, A. Kreter, B. Unterberg, Ch. Linsmeier

Forschungszentrum Jülich GmbH, Institut für Energie- und Klimaforschung – Plasmaphysik, Partner of the Trilateral Euregio Cluster (TEC), 52425 Jülich, Germany

ARTICLE INFO

Keywords: ITER grade 316L(N)-IG steel Deuterium plasma exposure Hydrogen permeation and retention Gas-driven deuterium permeation measurement Thermal desorption spectroscopy Surface roughness

ABSTRACT

Fuel permeation and retention in fusion reactor wall materials are important issues for plasma operation and safety reasons in ITER. The austenitic stainless steel 316L(N)-IG will be used as structural material in the first wall components in ITER. The impact of deuterium plasma exposure on the deuterium permeation and retention was studied. Polished 316L(N)-IG steel samples were deuterium plasma exposed with an ion energy of 200 eV and at two different fluences. Deuterium gas-driven permeation and thermal desorption spectroscopy measurements were performed afterwards. By comparison of the exposed samples to an unexposed sample, it is concluded that the surface roughness due to plasma exposure has no significant influence on the deuterium permeation through the samples. The first results of thermal desorption spectroscopy analysis show that the main release of retained deuterium is between 600°C and 900°C and the release temperature increases by increasing the plasma fluence.

1. Introduction

In order to make a reliable estimation of fuel loss and fuel inventory in the wall in ITER the deuterium retention and permeation through the 316L(N)-IG (316L) steel was studied. The fuel loss and inventory are especially important for safety reasons [1,2]. Furthermore, these parameters are necessary for the estimation of fuel recycling, which could have a significant impact on the operation performance [1]. This specially developed 316L steel [3] will be used as structure material in the first wall and in the ports in the ITER device. Although it is not foreseen that 316L will come in direct contact with the plasma, high energetic neutral particles can impinge the steel surface in the ports and in gaps between the tiles. It was estimated that the affected steel area is at least 8% of the total surface area of the vessel in ITER [4].

With the assumption, that the impact of the high energetic neutral particles is equal to the impact of deuterium plasma, polished 316L samples were exposed in the linear plasma device PSI-2 [5] and investigated afterwards. Detailed studies of the deuterium permeation through polished 316L and the influence of technical surfaces on the permeation can be found in [6]. It was shown in this publication that by roughening the surface by a specific grinding procedure, the permeation flux is slightly decreased by less than an order of magnitude compared to a polished sample. The conclusion was, that in the smear layer, which was produced by the grinding procedure, the permeation is smaller than in the bulk and that this is the main reason for the decrease of permeation flux. It was calculated that the influence of a

rough surface on the hydrogen permeation is very dependent on the roughness characteristics [7]. Therefore, this study aims to determine if the surface roughness produced by plasma exposure has an influence on the hydrogen permeation flux and the hydrogen retention. Since the neutral particle energies and fluxes at the above mentioned positions in ITER are only rough estimations [2], the ion energy was set around 200 eV, which is below the sputter threshold energy for deuterium on tungsten [8]. In order to study the influence of the plasma ion fluence on the studied characteristics, the plasma exposure took place with two different fluences, which are in the ITER relevant parameter regime [9]. The ion flux was set to around $3 \cdot 10^{21}$ ions/(m²s) and the different fluences were obtained by varying the exposure time. The first exposures took place with a tungsten sample holder mask. After the detection of tungsten contaminations on the plasma treated sample surfaces, which lead to a change in the deuterium permeation, the exposure and permeation measurement of the high fluence sample was repeated by using a steel mask (316Ti) during exposure. The results are compared with each other and to an unexposed sample.

2. Sample preparation and methods

All samples have a disk shape with a diameter of 24 mm, a thickness of 0.3 mm and were ground and polished to a mirror finish on both sides. The last polishing step was with a 1 μm diamond suspension and

E-mail address: an.houben@fz-juelich.de (A. Houben).

^{*} Corresponding author.

a cleaning with an oxide polishing suspension was applied afterwards. Before exposure, the samples were annealed at 570°C oven temperature (sample temperature around 550°C) for 2 h in a vacuum oven. In order to study the samples by different methods, we aimed to obtain four identical samples for each fluence. Since only two samples of this size can be exposed simultaneously in PSI-2, we performed two exposures per fluence. It is assumed that the resulted four samples for each fluence are identical and for each measurement method, a separate sample of these four samples is used. The plasma incident ion energy was 200 eV and the fluences were chosen to be $1 \cdot 10^{25}$ ions/m² (low fluence) and $5 \cdot 10^{25}$ ions/m² (high fluence). The samples were heated by the plasma beam to around 400°C during exposure. Pure deuterium gas (purity: 99.8%) was used for the plasma generation. In the used standard discharge regime, more than 90% of the ion flux is carried by D+ ions [10] and the sample area is exposed with an almost monoenergetic distribution of the incident ions [11]. In order to fix the samples on the sample holder plate, a tungsten sample mask was chosen, because the deuterium plasma energy was below the sputtering threshold energy of deuterium on tungsten, which is around 250 eV [8]. However, due to oxygen impurities in the plasma [12], the tungsten was sputtered and a slight tungsten contamination was detected on the surface of the plasma treated samples. Since these contaminations have influences on the deuterium permeation, the high fluence exposure was repeated by using a steel mask and no tungsten contamination was detected afterwards on this plasma exposed sample.

Four different sample kinds were investigated with the following methods and the results were compared: (1) reference sample: a polished 316L sample substrate (named '316L_sub'); (2) a 316L sample substrate plasma exposed after polishing and annealing in vacuum with an incident ion energy of 200 eV and a fluence of $1 \cdot 10^{25}$ ions/m² by using a tungsten sample holder mask (named '316L_LF'); (3) a 316L sample substrate plasma exposed after polishing and annealing in vacuum with an incident ion energy of 200 eV and a fluence of 5 · 10²⁵ ions/m² by using a tungsten sample holder mask (named '316L_HF'); (4) a 316L sample substrate plasma exposed after polishing and annealing in vacuum with an incident ion energy of 200 eV and a fluence of $5 \cdot 10^{25}$ ions/m² by using a steel sample holder mask (named '316L HF steel'). The reference sample (316L sub) substrates were annealed before permeation measurement, but not before the thermal desorption measurement in order to identify the native hydrogen content.

All samples were analyzed by scanning electron microscopy (SEM) using a Zeiss Crossbeam 540, equipped with a focused ion beam (FIB) and energy dispersive X-ray spectroscopy (EDX, Oxford X-Max 80, electron beam energy 5 keV). A cross section was created by the FIB enabling a side view of the sample surface. All surface SEM figures shown were recorded in SE mode, SEM on cross sections are recorded in the InLense mode. EDX measurement was used for elemental analysis.

The deuterium gas permeation setup consists of two volumes, the high and low pressure volume (HPV/LPV). The volumes are separated by the sample, which can be heated by a surrounding tube furnace. The base pressure of both volumes is in the 10^{-9} mbar range. In the HPV deuterium gas can be inserted and in the LPV the permeation flux is detected by a quadrupole mass spectrometer. Details of the setup can be found in [13]. The signal of the mass spectrometer was calibrated to a deuterium flux by four calibration leaks (LACO Technologies). Identical measurement cycles were performed on both samples. Each cycle consist of seven temperature steps in the indicated order: 'up'measurements: 300°C, 400°C, 500°C, 550°C; 'down'-measurements: 500°C, 400°C, 300°C. This measurement procedure was chosen in order to identify, if the sample characteristics change during permeation measurements. Exemplary, an increase of the permeation flux between the 'up' and 'down' measurement can be due to a filling effect, as observed in porous Y₂O₃ layers [13], or a reduction of a surface contamination, whereas an oxidation of the surface during measurement would lead to a decrease of the permeation flux [6]. After

stabilizing the sample at a specific temperature, the deuterium pressure was increased in six steps between 25 mbar and 800 mbar. Details of the lag-time measurements, which give information about the diffusion constant and activation energy, can be found in [6].

The thermal desorption spectroscopy (TDS) analysis measurements were performed between room temperature and 1000°C with a heating rate of 0.17 K/s. For comparison of the results, the span of time between exposure and TDS measurement was around one week and was very similar for all studied samples. The base pressure was in the order of 10^{-8} mbar and the heating rate is constant in the range between 200°C and 900°C. The desorbed specimens were detected by a quadrupole mass spectrometer (Pfeiffer, Prisma Plus) between 1 and 50 amu. The mass spectrometer signal was calibrated by pure hydrogen and deuterium gas with a constant and well defined flux for H₂ and D₂ with a calibration leak capillary tube. Due to the lack of HD gas for calibration, the mean value of H2 and D2 calibration results was taken for the HD signal calibration. The temperature given in the following is measured by a thermocouple in the middle of the vacuum tube at a thermally identical spot as the sample position. TDS measurements were performed on all samples, except the 316L_HF_steel sample, because we do not expect a measurable influence on the TDS results due to the slight tungsten contamination.

3. Data analysis

Details on the data analysis for the permeation measurement can be found in [6]. As explained above, all permeation measurements were performed by variation of deuterium pressure and sample temperature. In the diffusion-limited regime, the permeation flux can be expressed by [14.15]

$$J_P = \frac{P_0 \sqrt{p}}{d} e^{\frac{-E_P}{RT}} \tag{1}$$

wherein P_0 and E_P are the permeation constant and activation energy, p is the applied deuterium pressure, d is the thickness of the sample, R is the ideal gas constant and T the temperature. From the pressure dependence, the limiting regime for the permeation flux can be obtained. If the surface processes are quick with respect to the diffusion process, the permeation process is diffusion-limited. In this case the permeation flux is proportional to the square root of the applied deuterium pressure. In case of slow surface processes regarding the diffusion, the permeation process is surface-limited and the permeation flux is linearly proportional to the applied pressure. By varying the sample temperature, the permeation activation energy and constant can be obtained from the Arrhenius equation, if the data fulfill the equation. From the lag-time measurements and if the hydrogen permeation in the sample is limited by diffusion, the diffusion energy and constants can be determined [6].

The released hydrogen contents (H_2 , HD and D_2) of the samples were determined after background subtraction and signal calibration of the corresponding spectrum by integration of the peak areas. The hydrogen release temperature is not only dependent on the hydrogen trapping energy but also on other processes, like hydrogen diffusion and recombination. Since it is not possible to vary the heating rate in the current device, the trapping energies cannot be calculated from the obtained data. Nevertheless, by assuming that all other processes stays constant after sample treatment, the hydrogen release temperatures in the samples can be analyzed and compared.

4. Results

All samples were analyzed by SEM(FIB), as described above. On the unexposed 316L_sub sample a smooth surface with no smear layer was observed with SEM in the cross section (FIB) on both sides, see Fig. 1a. Due to the plasma treatment, a needle like structure was created on the plasma exposed side. The high fluence 316L_HF sample shows a much

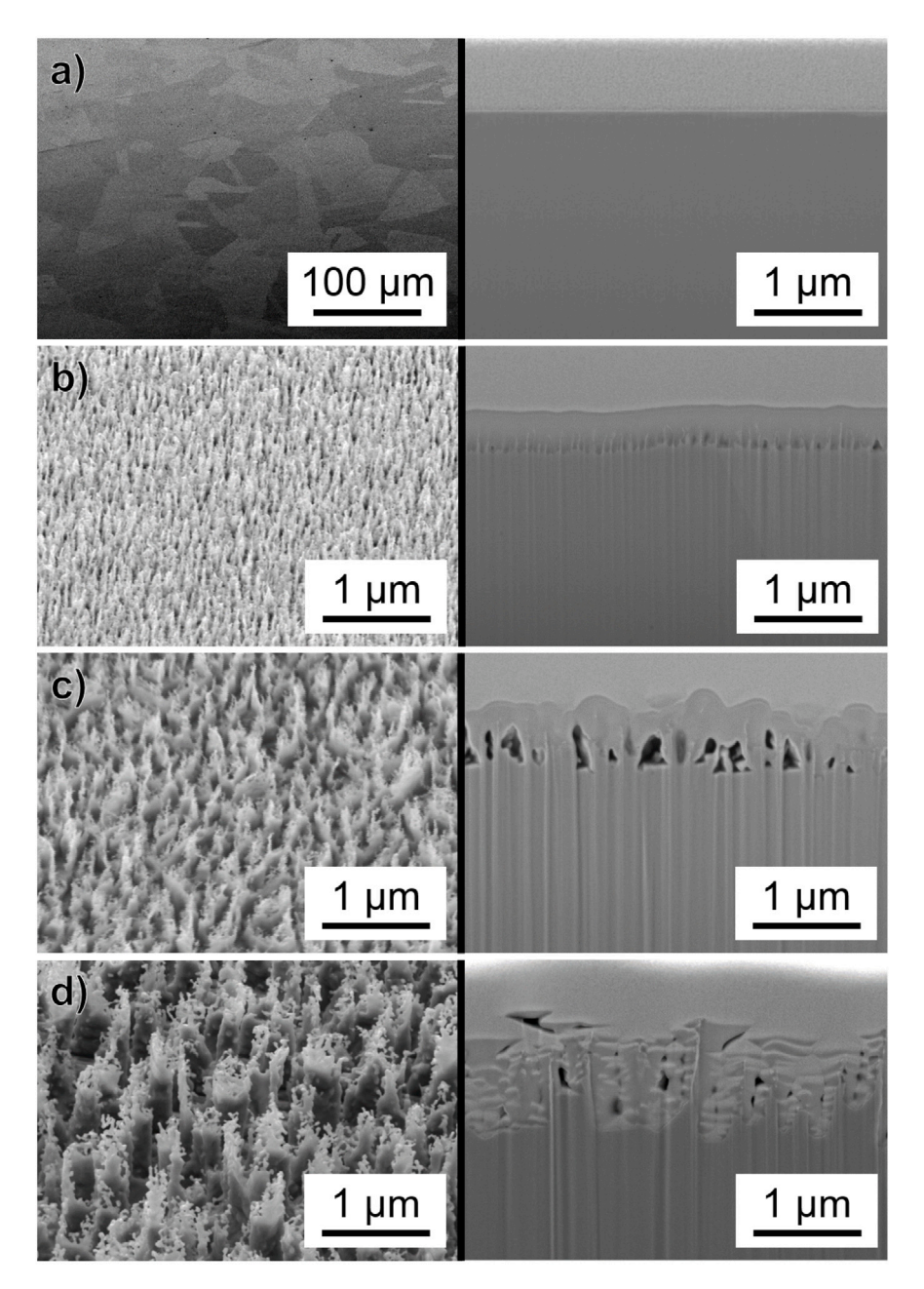


Fig. 1. SEM figures on left side show the top view and figures on the right side SEM on a cross section prepared by FIB. (a) polished 316L_sub sample (b) low fluence 316L_LF sample (c) high fluence 316L_HF sample (d) high fluence steel mask 316L_HF_steel sample. The bright area at the top of the SEM on the cross section figures (right) is a platinum layer applied for FIB cutting. The pores visible in the exposed samples, especially in the high fluence samples in figure c and d (right) are artifacts due to not complete enclosure of the surface characteristics with the applied platinum layer. The vertical line structure seen in the cross sections of the exposed samples are due to curtaining effect during cross sample preparation. Both artifacts are not due to the surface characteristics of the samples but due to cross section preparation.

coarser structure as the low fluence 316L_LF sample, as can be seen in Fig. 1b and c. The surface roughness of the 316L_HF_steel sample is shown in 1d. The surface roughness is similar to the 316L_HF sample surface roughness with a slightly different structure. After permeation measurements, the same analysis was performed on some samples, not shown, but no differences in the surface roughnesses were observed.

The surface composition in all samples was analyzed using EDX and the weight percent of the main elements can be found in Table 1. For comparison, the unexposed substrate sample was investigated as well and the values correspond to the company certificate. For the exposed samples, the investigation took place in the middle of the exposed surface area. The tungsten contamination in the 316L_LF and 316L_HF is coming from the tungsten mask used during exposure, because no

Table 1The results obtained from EDX measurements in the middle of the exposed surface area. The values are in weight percent. The errors are indicated in brackets.

Sample	Fe [wg%]	Cr [wg%]	Ni [wg%]	Mo [wg%]	O [wg%]	W [wg%]
316L_sub	65(1)	18(1)	12(1)	2(1)	-	-
316L_LF	58(1)	16(1)	12(1)	8(1)	2(1)	4(1)
316L_HF	57(1)	15(1)	10(1)	12(1)	2(1)	4(1)
316L_HF_steel	53(1)	15(1)	10(1)	20(1)	2(1)	-

tungsten is contained in the 316L steel. Since the exposure took place below the sputter threshold energy of deuterium on tungsten, the assumption is that the reason for the tungsten mask sputtering is the oxygen impurity in the deuterium plasma which is assumed [12] to

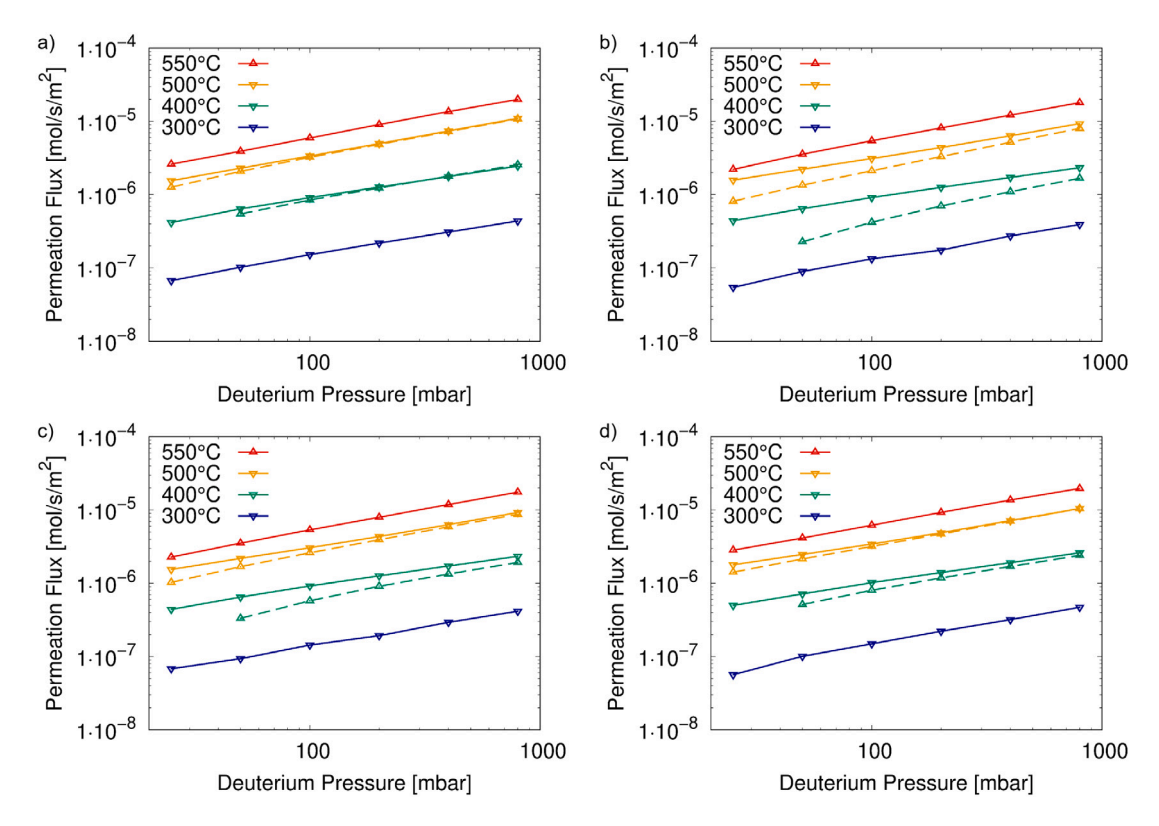


Fig. 2. Deuterium permeation flux through: (a) the polished and unexposed 316L_sub sample; (b) the low fluence 316L_LF sample; (c) the high fluence 316L_HF sample; (d) the high fluence steel mask 316L_HF_steel sample. The dotted lines with the up-arrows indicates the 'up'-measurements, see text, the solid lines with the down-arrows indicate the 'down'-measurements.

Table 2 The results obtained from temperature and pressure dependent permeation measurements (x, P_0, E_P) . The values for the unexposed sample 316L_sub 'down' are from reference [6]. The data for the 'up'-measurement are derived from the data at 400°C (slope) and 400 mbar $(E_P \text{ and } P_0)$. The errors are indicated in brackets.

Sample	p^x	$P_0 \left[rac{ ext{mol}}{ ext{ms} \sqrt{ ext{mbar}}} ight]$	$E_P\left[\frac{\mathrm{kJ}}{\mathrm{mol}}\right]$
316L_sub, 'up' 316L sub, 'down' [6]	0.58(2) 0.5	$19(1) \cdot 10^{-7} \\ 8(1) \cdot 10^{-7}$	62(1) 58(1)
316L_LF, 'up'	0.75(4)	$70(1) \cdot 10^{-7}$	73(1)
316L_LF, 'down'	0.50(1)	$10(2) \cdot 10^{-7}$	59(1)
316L_HF, 'up'	0.66(4)	$30(1) \cdot 10^{-7}$	67(1)
316L_HF, 'down'	0.50(2)	$7(1) \cdot 10^{-7}$	58(1)
316L_HF_steel, 'up'	0.58(2)	$19(1) \cdot 10^{-7}$	63(1)
316L_HF_steel, 'down'	0.50(2)	$9(1) \cdot 10^{-7}$	58(1)

be about 0.2%. The sputter threshold energy for oxygen on tungsten is much lower as for deuterium on tungsten [8]. We assume that the tungsten contamination is oxidized and exist as tungsten oxide on the surface. It has to be noted that it is not possible with EDX to quantify the amount of this thin layer of tungsten oxide, since EDX is not surface sensitive. Therefore, the tungsten and oxygen values in Table 1 have to be interpreted carefully. In the 316L_HF_steel sample, no tungsten contamination was observed. Due to the fact that the deuterium ion sputter threshold energy is lower and the sputter yield is higher for iron than for molybdenum at 200 eV ion energy [8], the iron is preferentially sputtered. Therefore, the Mo content is larger in the plasma exposed samples than in the unexposed sample, especially in the 316L_HF_steel sample. Furthermore, in the samples with the tungsten contamination, the preferential sputtering of Fe is lower compared to the 316L_HF_steel. The assumption is that the W contamination reduces the iron sputtering.

The comparison of the permeation flux versus the applied deuterium pressure of the unexposed 316L_sub (a), the low fluence 316L_LF (b), the high fluence 316L_HF (c) and the 316L_HF_steel (d) samples is

shown in Fig. 2. In all 300°C 'up'-measurements and in the 25 mbar at 400°C 'up'-measurements, the permeation flux signal is low, unstable and in the low applied gas pressure range below the detection limit. That is why a reliable data analysis is not possible and therefore the data are neglected. In the exposed samples 316L_LF and 316L_HF a clear deviation between 'up'- and 'down'-measurements is observed, see Fig. 2b and c. These deviations indicate a change of sample characteristics during measurement. Due to this reason, the slope and the permeation activation energy is changing between 'up'- and 'down'-measurements and therefore in Table 2 the 'up' values at 400°C (slope) and 400 mbar (E_P and P_0) are given for all samples. In case of the 316L_HF_steel sample, the deviation between 'up'- and 'down'-measurements is small, see Fig. 2d and Table 2, and similar to the unexposed sample 316L sub.

The deuterium lag-time was measured for all samples after the permeation flux measurement. Since the exposed samples are stable after the permeation flux measurements and the behavior is comparable to the unexposed sample, the results of these lag-time measurements are identical for all samples. Details of the hydrogen diffusion through 316L steel can be found in [6].

The comparison of the TDS spectra of the released H_2 (a), HD (b) and D_2 (c) intensity of the unexposed, low and high fluence sample is shown in Fig. 3. The calibrated signals are shown after background subtraction. The hydrogen release of the unexposed 316L_sub sample (blue) corresponds to the native hydrogen content in the sample from production, because the sample was not annealed before measurement. The released deuterium inventory is higher than expected regarding the 0.01% fraction of deuterium in natural hydrogen, which is assumed to be due to an increased deuterium background in the chamber. As explained above, the exposed samples were annealed before the exposure in order to eliminate the native hydrogen content. In the low fluence 316L_LF sample (red), the annealing temperature was not high enough due to a problem with the temperature calibration of the oven, that is why there is H_2 release from remained native hydrogen,

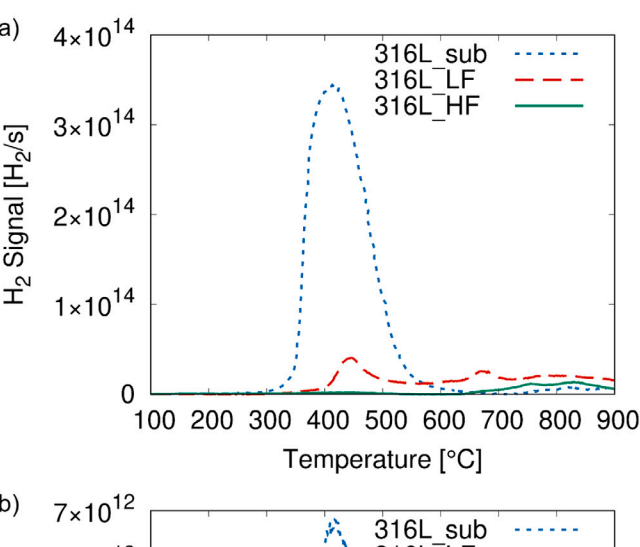
which can be seen between 400°C and 500°C in Fig. 3a. The HD signal shows also a peak in this temperature range, which we assume is also related to the remained native hydrogen. In the high fluence 316L_HF sample (green), the native hydrogen content was eliminated up to the annealing temperature of 570 °C before exposure. Due to the influence of the native hydrogen background, the determination of the released deuterium content for the low fluence sample is defective. Therefore, the comparison of the difference in the deuterium content form exposure between the high and low fluence sample is difficult. By integration of the area between 600°C and 900°C of the calibrated and background subtracted spectrum one obtain a deuterium content of $2.7\cdot10^{15}$ atoms and $2.1\cdot10^{15}$ atoms for the low and high fluence sample, respectively. In this calculation also the deuterium part in the HD signal was included.

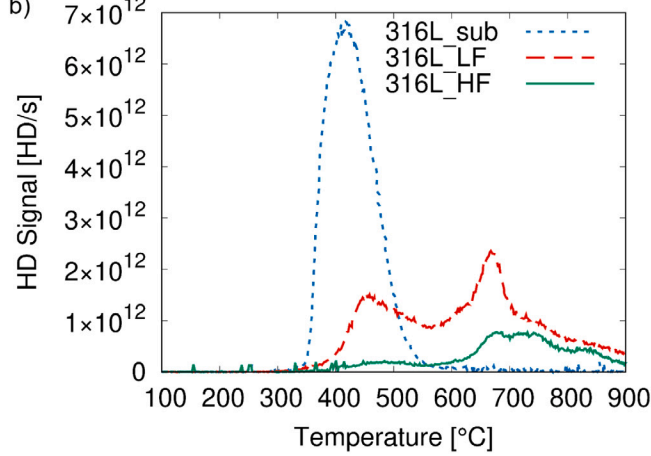
5. Discussion

The comparison of the permeation flux versus the applied pressure of the 316L LF and the 316L HF samples in Fig. 2b and c shows, that the permeation behavior is very similar in both samples. In the 'up'measurement a lower permeation flux is measured compared to the 'down'-measurement. In Table 2 the slope of the 'up'-measurements is between 0.5 and 1 which indicate an influence of the surface processes. In the 'down'-measurements of both samples, the slope is 0.5, which indicates a pure diffusion-limited deuterium permeation process and the permeation activation energy and constant is identical to the unexposed sample. In case of the 316L_HF_steel sample the deviation between the 'up' and the 'down' measurement is small and similar to the deviation in the unexposed sample 316L sub. From these observations it is concluded, that the contamination on the 316L_LF and the 316L_HF samples is tungsten oxide. This contamination acts as a permeation barrier during the 'up'-measurement. Since tungsten oxide, in opposite to non-oxidized tungsten, is reduced by the applied temperature and deuterium atmosphere [16] during the 'up' measurement, the permeation flux in the 'down' measurement is higher. Therefore, the deviation between the 'up'- and the 'down'-measurements in the plasma exposed samples by using the tungsten mask is larger compared to the plasma exposed sample using the steel mask 316L HF steel. Since the surface roughnesses of all plasma exposed samples are not changed by the permeation measurement and the results of the 'down'-measurements are very similar to the unexposed sample, the surface roughness due to plasma exposure has no influence on the deuterium permeation through these samples.

The results of the lag-time measurements, which were performed after annealing the sample in deuterium, see above, and hence the hydrogen diffusion through the samples are identical to the polished sample. This is in disagreement to the measurement result of the rough 316L sample in [6], where it was found, that the diffusion activation energy and the diffusion constant is lowered by the surface treatment. Since the influence of the surface on the diffusion is related to the smear layer on the rough sample in [6], the conclusion is, that the 'pure' roughness without smear layer obtained by plasma exposure does not lead to an influence of the deuterium diffusion in the samples. Furthermore, this conclusion is confirmed by the result, that the permeation process is diffusion limited in all 'down'-measurements, see Table 2, meaning that the surface processes are fast and do not hinder the permeation process.

In the TDS measurements of the unexposed sample in Fig. 3 the main release of the native hydrogen (H_2 , HD, D_2) is detected around 400°C as a single peak. The deuterium which was implanted during plasma exposure is released at higher temperatures in the range between 600°C and 900°C. In the released deuterium signal (Fig. 3c) double or triple peak structure can be observed which shifts to higher temperatures with increasing fluence. The fluence dependence can be due to the following reasons: (1) the deuterium diffuses deeper into the sample with increased fluence, which leads to a longer time until





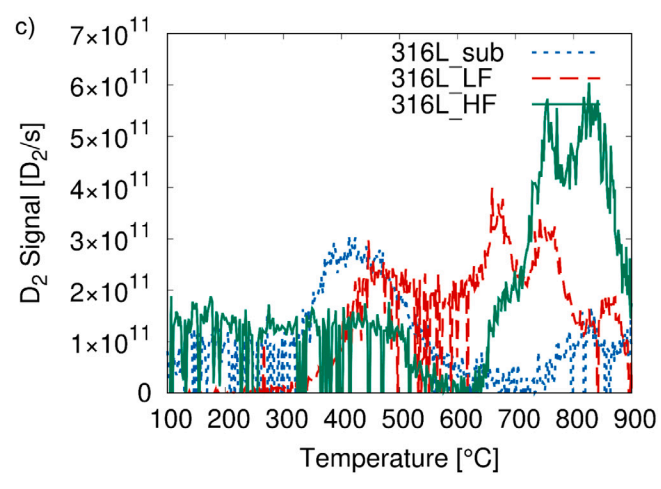


Fig. 3. Released gas signal versus applied temperature from the unexposed sample $316L_sub$ (blue), the low fluence sample $316L_sub$ (red) and the high fluence sample $316L_sub$ (green). In figure (a) the H_2 signal, (b) the HD signal, and (c) the D_2 signal is shown. The calibrated signals are shown after background subtraction.

the deuterium reach the surface and can be released; (2) the hydrogen recombination at the surface or the diffusion through the surface contamination and roughness is different in the exposed samples due to the much coarser structure in the high fluence sample; (3) the trapping energy or trap density is increased with increase of the deuterium fluence. Due to the fact that the sample is very thin and the diffusion is high, reason one is unlikely. Since the permeation flux measurements indicate that the hydrogen recombination and diffusion are not influenced by the different surface characteristics of the samples, reason two

is not obvious. To understand this behavior further TDS measurements have to be performed with varying heating rate.

In the comparison of the deuterium content in the samples, the high fluence sample shows a smaller deuterium content as the low fluence sample, which is contradictory to an intuitive assumption. As explained above, the deuterium content in the low fluence sample is defective due to the large hydrogen background. Furthermore, the TDS measurements stopped around 1000°C. Since the release temperature is increased by increasing the fluence, more deuterium could be released in the high fluence sample if the measurement would be extended to higher temperatures.

6. Conclusions and outlook

Polished 316L(N)-IG samples were exposed to a 200 eV deuterium plasma in the linear plasma device PSI-2 with two different fluences. The obtained needle like structure on the exposed sample surface is coarser with higher fluence. The permeation behavior is similar in all three kinds of exposed samples and an unexposed sample. The conclusion is that the roughness of the surface due to plasma exposure does not have an influence on the permeation flux or hydrogen diffusion. The tungsten oxide contamination on two kinds of these samples is due to oxygen impurities in the plasma which sputter the tungsten mask. The tungsten oxide contamination acts as a permeation barrier and decreases the permeation flux. After annealing at 550°C in a deuterium atmosphere during permeation measurements, the tungsten oxide contamination is reduced, the permeation flux is increased, stabilized and identical to the unexposed sample. In the TDS measurements, the implanted deuterium is released between 600°C and 900°C. The high fluence sample shows a higher release temperature as the low

Further measurements will be performed at a lower plasma energy in order to study the influence of the incident ion energy. In order to study the influence of plasma induced surface roughness on the hydrogen permeation further, samples will be exposed under different plasma conditions in order to vary the surface roughness. TDS measurements with varying heating rates will be performed in order to understand the influence of the deuterium plasma fluence.

CRediT authorship contribution statement

A. Houben: Conceptualization, Methodology, Formal analysis, Investigation, Writing - original draft, Visualization. J. Scheuer: Investigation. M. Rasiński: Investigation, Formal analysis. A. Kreter: Methodology, Investigation. B. Unterberg: Project administration. Ch. Linsmeier: Conceptualization, Resources, Writing - review & editing, Funding acquisition.

Declaration of competing interest

The authors declare that they have no known competing financial interests or personal relationships that could have appeared to influence the work reported in this paper.

Acknowledgments

The authors thank G. De Temmerman for providing the 316L(N)-IG sample material and B. Göths for sample preparation. A part of this work has been carried out within the framework of the EUROfusion Consortium (WP PFC) and has received funding from the Euratom research and training program 2014–2018 and 2019–2020 under grant agreement No 633053. The views and options expressed herein do not necessarily reflect those of the European Commission.

References

- [1] R.A. Causey, J. Nucl. Mater. 300 (2) (2002) 91-117.
- [2] J. Roth, E. Tsitrone, A. Loarte, T. Loarer, G. Counsell, R. Neu, V. Philipps, S. Brezinsek, M. Lehnen, P. Coad, C. Grisolia, K. Schmid, K. Krieger, A. Kallenbach, B. Lipschultz, R. Doerner, R. Causey, V. Alimov, W. Shu, O. Ogorodnikova, A. Kirschner, G. Federici, A. Kukushkin, J. Nucl. Mater. 390–391 (2009) 1–9, Proceedings of the 18th International Conference on Plasma-Surface Interactions in Controlled Fusion Device.
- [3] G. Wille, K. Slattery, D. Driemeyer, G. Morgan, Fusion Eng. Des. 39–40 (1998) 499–504.
- [4] J. Romazanov, S. Brezinsek, A. Kirschner, A. Eksaeva, D. Borodin, R.A. Pitts, E. Veshchev, V.S. Neverov, A.B. Kukushkin, A.G. Alekseev, C. Linsmeier, Nucl. Fusion (2021) in preparation.
- [5] A. Kreter, C. Brandt, A. Huber, S. Kraus, S. Möller, M. Reinhart, B. Schweer, G. Sergienko, B. Unterberg, Fusion Sci. Technol. 68 (1) (2015) 8–14, http://dx.doi.org/10.13182/FST14-906.
- [6] A. Houben, J. Engels, M. Rasiński, C. Linsmeier, Nucl. Mater. Energy 19 (2019) 55–58
- [7] A. Pisarev, I. Tsvetkov, S. Yarko, T. Tanabe, AIP Conf. Proc. 837 (1) (2006) 238–249, https://aip.scitation.org/doi/abs/10.1063/1.2213079.
- [8] R. Behrisch, W. Eckstein, in: R. Behrisch, W. Eckstein (Eds.), Sputtering by Particle Bombardment, in: Topics in Applied Physics, vol. 110, Springer-Verlag Berlin Heidelberg, 2007.
- [9] R. Behrisch, G. Federici, A. Kukushkin, D. Reiter, J. Nucl. Mater. 313–316 (2003) 388–392. Plasma-Surface Interactions in Controlled Fusion Devices 15.
- [10] I. Sorokin, I. Vizgalov, V. Kurnaev, C. Brandt, A. Kreter, C. Linsmeier, Nucl. Mater. Energy 12 (2017) 1243–1247, Proceedings of the 22nd International Conference on Plasma Surface Interactions 2016, 22nd PSI.
- [11] C. Linsmeier, B. Unterberg, J. Coenen, R. Doerner, H. Greuner, A. Kreter, J. Linke, H. Maier, Nucl. Fusion 57 (9) (2017) 092012.
- [12] J. Schmitz, A. Litnovsky, F. Klein, T. Wegener, X. Tan, M. Rasinski, A. Mutzke, P. Hansen, A. Kreter, A. Pospieszczyk, S. Möller, J. Coenen, C. Linsmeier, U. Breuer, J. Gonzalez-Julian, M. Bram, Nucl. Mater. Energy 15 (2018) 220–225.
- [13] J. Engels, A. Houben, M. Rasinski, C. Linsmeier, Fusion Eng. Des. 124 (2017) 1140–1143.
- [14] R. Causey, R. Karnesky, C.S. Marchi, in: R.J. Konings (Ed.), Comprehensive Nuclear Materials, Elsevier, Oxford, 2012, pp. 511–549.
- [15] C. Linsmeier, M. Rieth, J. Aktaa, T. Chikada, A. Hoffmann, J. Hoffmann, A. Houben, H. Kurishita, X. Jin, M. Li, A. Litnovsky, S. Matsuo, A. von Müller, V. Nikolic, T. Palacios, R. Pippan, D. Qu, J. Reiser, J. Riesch, T. Shikama, R. Stieglitz, T. Weber, S. Wurster, J.-H. You, Z. Zhou, Nucl. Fusion 57 (9) (2017) 092007
- [16] J.W. Coenen, G.D. Temmerman, G. Federici, V. Philipps, G. Sergienko, G. Strohmayer, A. Terra, B. Unterberg, T. Wegener, D.C.M.V. den Bekerom, Phys. Scr. T159 (2014) 014037.